

VII International Conference on Computational Plasticity
COMPLAS 2003
E. Oñate and D.R.J. Owen (Eds)
©CIMNE, Barcelona, 2003

DISCONTINUITIES IN REGULARISED MEDIA

Angelo Simone, Garth N. Wells and Lambertus J. Sluys

Delft University of Technology
Faculty of Civil Engineering and Geosciences
P.O. Box 5048, 2600 GA Delft, The Netherlands
Emails: a.simone@citg.tudelft.nl, g.wells@citg.tudelft.nl, l.j.sluys@citg.tudelft.nl

Key words: Fracture, Damage, Plasticity, Rate-dependent media, Gradient-enhanced media, Discontinuities.

Abstract. *Discontinuous interpolation of the problem fields in non-local and rate-dependent media is considered. The necessity of discontinuities in the analysis of failure processes and some of the requirements for the introduction of discontinuities in regularised media are discussed. The regularisation properties of a novel rate-dependent elastoplastic damage continuum model are presented.*

1 INTRODUCTION

The analysis of failure processes by means of numerical techniques in which discontinuities in the problem fields are allowed may lead to a more realistic representation of the involved processes up to complete failure. Failure can then be realistically described as progressive material degradation which develops into a discrete crack, for which a discontinuity in the displacement field is a suitable representation [1, 2]. In a phenomenological description of failure in quasi-brittle materials, strain-softening relationships are exploited to describe the progressive loss of load-carrying capacity in a continuous setting. In that case, regularisation techniques must then be included in the constitutive relationships in order to obtain mesh objectivity.

This paper focuses on the inclusion of discontinuities in regularised media. Some issues related to the discontinuous enrichment in regularised media are addressed by analysing the impact of a discontinuous interpolation of the problem fields on two kinds of regularised model: a non-local damage and a rate-dependent elastoplastic damage model. Through a discontinuous interpolation of local and non-local kinematics of a gradient-enhanced continuum damage model, spurious damage growth close to complete failure can be avoided. However, due to the non-local regularisation, the response of the model to the enhancement can be problematic [3]. When a discontinuous interpolation is considered in a rate-dependent elastoplastic damage model, the model predicts results which are closer to the physical reality than the continuum model alone.

2 ESSENTIALS OF THE COMPUTATIONAL FRAMEWORK

A brief description of the constitutive relationships is given next along with the technique used to incorporate discontinuities in the kinematic fields.

2.1 Constitutive relationships

Common to the two classes of regularised constitutive models considered here is the use of the damage framework to represent void development. The damage model is assumed to be isotropic, with degradation described by a scalar variable ω ranging from 0 (virgin material) to 1 (total loss of coherence). The effective stress tensor $\tilde{\boldsymbol{\sigma}}$ is related to the homogenised stress tensor $\boldsymbol{\sigma}$ and to the elastic strain tensor $\boldsymbol{\varepsilon}^e$ through

$$\tilde{\boldsymbol{\sigma}} = \frac{\boldsymbol{\sigma}}{1 - \omega} = \mathbf{D}^e : \boldsymbol{\varepsilon}^e, \quad (1)$$

where \mathbf{D}^e is the fourth-order elastic stiffness tensor. To avoid mesh dependence, damage evolution must be postulated as some function of a regularised monotonically increasing deformation history invariant κ . For the gradient-enhanced continuum damage model, damage evolution is made a function of the non-local equivalent strain, while in the rate-dependent elastoplastic damage model, damage is made a function of the equivalent viscoplastic strain. The two frameworks differ significantly in the nature of the regularisation involved (temporal regularisation *versus* spatial regularisation) and in the dissipation

mechanism. It is noted that in the rate-dependent elastoplastic damage model, damage is plastically-induced.

In the gradient-enhanced continuum damage model, damage evolution can be described by using an exponential softening law [4]:

$$\omega = \begin{cases} 0 & \text{if } \kappa \leq \kappa_0 \\ 1 - \frac{\kappa_0}{\kappa} (1 - \alpha + \alpha \exp(-\beta(\kappa - \kappa_0))) & \text{if } \kappa > \kappa_0, \end{cases} \quad (2)$$

or by a modified power softening law [5]:

$$\omega = \begin{cases} 0 & \text{if } \kappa \leq \kappa_0 \\ 1 - \left(\frac{\kappa_0}{\kappa}\right)^\beta \left(\frac{\kappa_c - \kappa}{\kappa_c - \kappa_0}\right)^\alpha & \text{if } \kappa_0 \leq \kappa < \kappa_c \\ 1 & \text{if } \kappa \geq \kappa_c, \end{cases} \quad (3)$$

with α and β model parameters, κ_0 the threshold for damage initiation and κ_c the value of the history parameter κ for which damage reaches unity. In the rate-dependent elastoplastic damage model, damage evolution is postulated as:

$$\omega = \begin{cases} 0 & \text{if } \kappa \leq \kappa_0 \\ \alpha (1 - \exp(-\beta\kappa)) & \text{if } \kappa > \kappa_0, \end{cases} \quad (4)$$

with α and β model parameters and κ_0 the converged value of the equivalent plastic strain from the previous step

The rate-dependent isotropic elastoplastic damage model is discussed in detail in Appendix A where the algorithmic treatment is presented and the regularisation properties are illustrated. Details of the implicit gradient-enhanced continuum damage model can be found in Ref. [4], for the regularisation properties of the continuum model, and in Ref. [3], for the transition from continuous to continuous/discontinuous failure description.

2.2 Discontinuous interpolation

The discrete representation of a discontinuity can be rigorously achieved through a discontinuous interpolation of the problem fields [1, 2]. For the body $\bar{\Omega}$ depicted in Figure 1, which is divided into two sub-domains ($\Omega = \Omega^+ \cup \Omega^-$) by a discontinuity surface Γ_d , the displacement field is given by

$$\mathbf{u} = \hat{\mathbf{u}} + \mathcal{H}_{\Gamma_d} \tilde{\mathbf{u}}, \quad (5)$$

where \mathcal{H}_{Γ_d} is the Heaviside function centred at the discontinuity surface ($\mathcal{H}_{\Gamma_d} = 1$ if $\mathbf{x} \in \bar{\Omega}^+$, $\mathcal{H}_{\Gamma_d} = 0$ if $\mathbf{x} \in \bar{\Omega}^-$) and $\hat{\mathbf{u}}$ and $\tilde{\mathbf{u}}$ are continuous functions on $\bar{\Omega}$. In a discretised framework, equation (5) can be written as [1, 2]

$$\mathbf{u}_h = \mathbf{N}\mathbf{a} + \mathcal{H}_{\Gamma_d} \mathbf{N}\mathbf{b}, \quad (6)$$

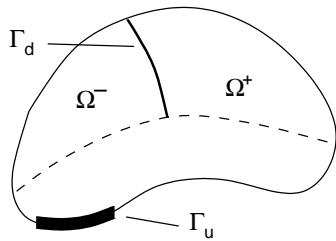


Figure 1: Body $\bar{\Omega}$ crossed by a discontinuity surface Γ_d .

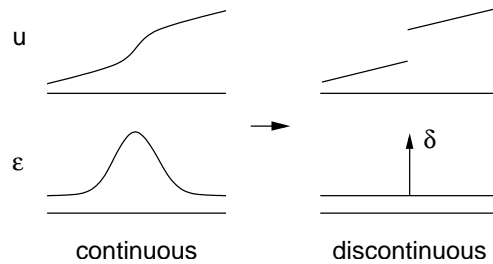


Figure 2: From continuous to discontinuous displacement/strain profiles as a consequence of strain localisation.

with \mathbf{N} a matrix containing standard finite-element shape functions and \mathbf{a} and \mathbf{b} vectors containing global degrees of freedom.

The inclusion of displacement discontinuities represents, in this context, genuine separation of materials—a discontinuity is extended when damage in all integration points in the element ahead of the discontinuity tip is above a critical value close to unity. Note that the inclusion of internal discontinuity surfaces in a finite-element is equivalent to the application of natural boundary conditions, without modifications of the original finite-element mesh, at the discontinuity surface. The introduction of a discontinuity at (almost) total loss of load-carrying capacity is in line with the narrowing of the strain profile as a consequence of strain localisation (cf Figure 2).

3 INTRODUCTION OF DISCONTINUITIES IN REGULARISED MEDIA

When introducing discontinuities in the problems fields, some requirements on the underlying continuum description must be satisfied. Obvious requirements are related to the nature of the continuum constitutive relationship which has to be properly regularised—numerical results must be *independent from mesh type, size and orientation* and the *failure mode must be physically reasonable* (the location of failure initiation and the evolution of failure should be correctly predicted). Less obvious requirements, but equally important, reside in the ability of the model to allow the formation of a *localised strain profile* with *full stress relaxation at significant deformation* and without *spurious degradation* close to failure for a correct description of a stress-free crack. A summary of the above requirements is shown in Table 1.

4 FROM A CONTINUOUS TO A CONTINUOUS/DISCONTINUOUS FAILURE REPRESENTATION

Failure representation in quasi-brittle materials makes use, in a continuous setting, of strain-softening constitutive relationships in which full stress relaxation is achieved at infinite strain values (cf Figure 3a). The reasons are of practical and of theoretical nature. This setting is a very convenient one since it allows numerical analyses to be performed in a

Table 1: Requirements for the introduction of discontinuities in regularised media

regularisation technique requirements	
1	physically reasonable failure mode
2	mesh type/size/orientation independence
failure representation requirements	
3	strain localisation
4	full stress relaxation at significant deformation
5	no spurious degradation close to failure

continuous framework. Using continuum damage softening constitutive relationships with full stress relaxation at significant strain values, like the one depicted in Figure 3b, poses the problem of dealing with damage values equal to unity (*i.e.* with a singular stiffness matrix). Considerations of theoretical nature lead to the conclusion that the asymptote of such constitutive relationships might be useful in reproducing the long tail observed in load-displacement diagrams of concrete specimens which is related to crack bridging. The above justifications assume that failure representation can be rigorously characterised in a continuous setting. However, this is not correct due to the inability of describing a kinematic discontinuity in the primal field in a continuous setting. Continuum damage or plasticity models are best suited for modelling diffuse microcracking, in strain-softening or -hardening materials, before macrocracks become dominant. A better approximation of failure processes can be achieved by using numerical techniques in which a discontinuity is naturally endowed in the model itself.

To illustrate one of the incongruities due to an erroneous use of strain-softening relationships, the normalised stress-strain softening paths for a one-dimensional uniform loading state field related to material data used in the analysis of a four-point bending test [6] (exponential softening law, equation (2)) and of a compact-tension test [7] (power softening law, equation (3)) are reported in Figure 3—the pictures depicted in Figure 3 are based on equation 1. For the exponential law (Figure 3a), an increment of less than 1% in damage requires an increment of approximately 512% in deformation which corresponds to a drop in the normalised stress of about 39%; for the power law (Figure 3b), only an increase of 23% in the deformation is necessary to drop the stress of about 88% for the same increment of damage. The physical relevance of exponential softening law with a high residual stress is questionable since it might alter the local/global level response. Conversely, the use of softening laws with a small residual stress (such that damage can reach values very close to unity) can be beneficial only in small scale analyses but its efficiency can be lost in large scale analyses due to the poor conditioning of the global system of equations. A similar situation occurs in softening plasticity when the loading function reduces to a point (with the von Mises yield criterion).

The use of constitutive laws with full stress relaxation at significant strain, or with a small residual stress when small scale analyses are considered, in conjunction with a

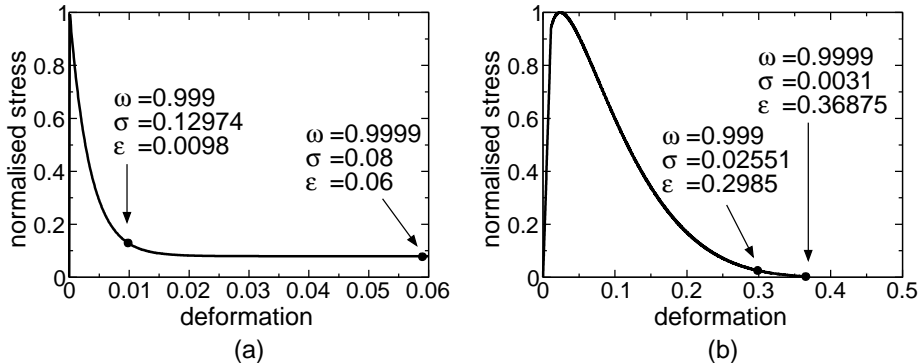


Figure 3: Stress-strain softening curves for exponential (a) and power (b) law of damage growth.

numerical technique in which the problem fields are allowed to develop a discontinuity, enables the more realistic description of failure.

5 FAILURE INITIATION AND NEAR-TIP FIELDS

Proper failure characterisation relies on correct failure initiation. In quasi-brittle analyses of notched specimens, experimental evidence shows that cracks propagate from the notch. Proper modelling of quasi-brittle material behaviour must reproduce this phenomenon.

In the computational framework used in this paper, a discontinuity propagates from an existing discontinuity which is present from the beginning of the analysis. When a non-local model [4, 8] is considered, it can be demonstrated that, due to non-local averaging near boundaries, failure initiation and characterisation is significantly changed. Simple analytical considerations, in the elastic regime and under the assumption of a plane stress situation, show that in a non-local damage model, for a single edge crack specimen with a sharp crack, damage initiation is predicted ahead of the crack tip and not at the crack tip. This shift in the location of damage initiation is proportional to the length scale parameter. Note that, in general, the use of non-local averaging of field quantities with isotropic weight functions results in a modification of failure characterisation. In the class of non-local elasticity models proposed by Eringen et al. [9], the stress field value at the crack tip is finite but, like the non-local damage model considered here, its maximum is at some distance from the crack tip. For the rate-dependent elastoplastic damage model described in Appendix A, analytical investigations of the near-tip fields behaviour are not available. Some analytical solutions are however known, under a certain number of assumptions, for simple constitutive relationships [10, 11]. Knowing that near-tip fields strongly depend on the assumed constitutive relationship, it is not possible to extend the results available from literature to the rate-dependent elastoplastic damage model considered here. Some numerical evidence suggests that, for strain-softening rate-dependent plastic-

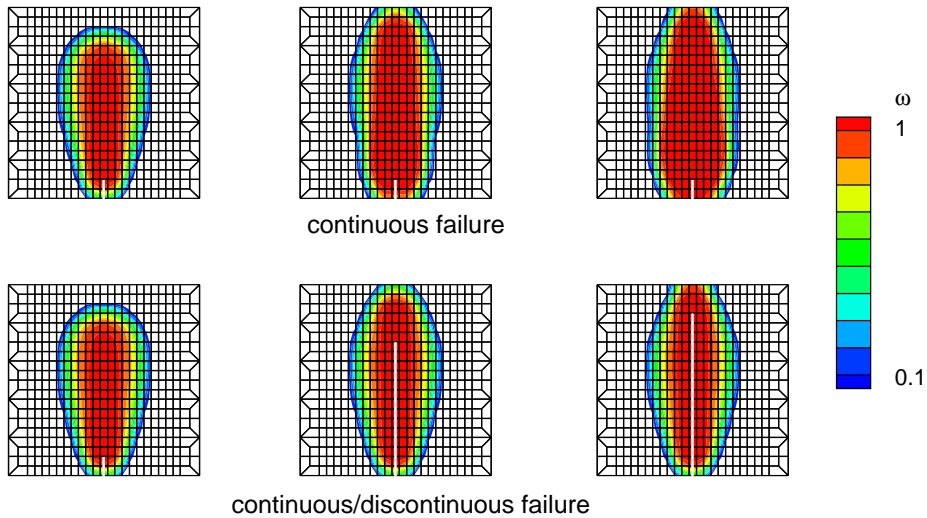


Figure 4: Effect of the inclusion of a discontinuity on the damage profile: damage evolution without (top) and with (bottom) a propagating discontinuity (close-up of the central part of a four-point bending specimen [3]; the discontinuity is represented by the white thick line).

ity (rate-dependence was introduced by means of Perzyna viscoplasticity with $N = 1$, cf equation (A.7), with a smoothed Rankine yield criterion under the assumption of a plane stress situation), the dissipation-driving field quantity is maximum, at the beginning of the dissipation process, at the crack-tip. Mesh refinement studies also indicated that the energy dissipated during a load process converges to a non-zero value. From here it can be concluded that the dissipation-driving field quantity converges to a finite value at the crack tip. These conclusions are based on numerical considerations and, as such, must be validated by analytical studies.

6 PROBLEM FIELDS CHARACTERISATION UPON DISCONTINUITY EXTENSION

A discontinuous problem field interpolation is intended to give a better failure representation. In the context of constitutive models for quasi-brittle materials, there are some regularised models in which the use of discontinuities may solve some problems inherent to the nature of the regularisation. This is the case for non-local regularisation in the format proposed by Pijaudier-Cabot and Bažant [8] and later reformulated by Peerlings et al. [4]. In that framework, due to non-local averaging of the field quantity driving damage evolution, damage growth is not correctly predicted [5] (cf. Figure 4, top). This problem has been solved by using a variable length scale [5] or by a discontinuous problem fields interpolation [3] (cf. Figure 4, bottom). The latter approach has been used, in a different context, by Jirásek and Zimmermann [12].

A fundamental question resides in the actual meaning of the inclusion of discontinuities (of any nature, cohesive or traction-free), which are local in space, in problem fields

which are, by definition, non-local. Some analyses performed with the implicit gradient-enhanced continuum damage model, whose results are reported in Figure 5a, showed how, of all the basic problem fields (vertical displacement field u_y and non-local equivalent strain field e), only the non-local strain field suffered from severe oscillations upon a discontinuity extension. Analogous analyses performed with the rate-dependent model described in Appendix A did not show oscillations for the equivalent plastic strain κ (cf Figure 5b).

Numerical evidence showed that the shift of the maximum of the non-local equivalent strain away from the crack-tip is even more pronounced in the non-linear regime than it is in the elastic regime. The consequence is that, for a reasonably fine discretisation, several elements are crossed at a time. The oscillations of the dissipation driving quantity are more pronounced by the release of more than one element at a time. This causes a situation of spurious unloading in the points ahead of the newly extended discontinuity tip resulting in the bumps in the load-displacement curve as depicted in Figure 6a. Note that this phenomenon is related to the resolution of the mesh with respect to the length scale—if a (too) coarse mesh is used it is likely that bumps in the load-displacement response will not appear. When the rate-dependent model described in Appendix A is considered, usually one element at a time is crossed by the discontinuity and the load-displacement curves do not show bumps (Figure 6b).

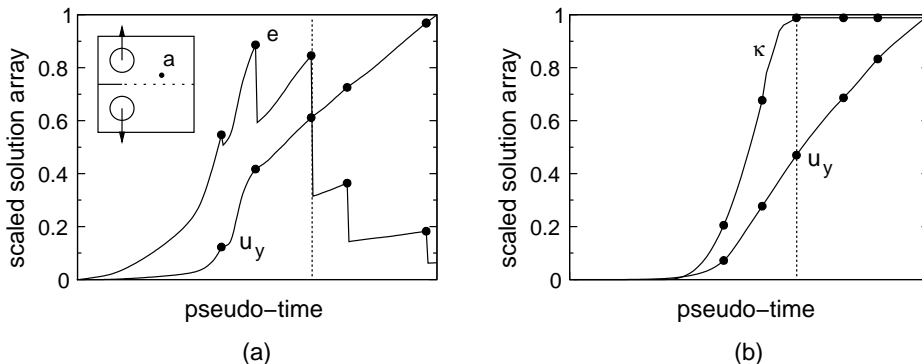


Figure 5: Pseudo-time evolution of the vertical displacement field and of the dissipation-driving quantity e for implicit gradient-enhanced continuum damage model (a) and of κ for the rate-dependent elastoplastic damage model (b) in a compact tension test for point a . The discontinuity propagates from the notch along the dotted line. The dots represent the extension of the discontinuity, one element at a time, and the dotted line indicates the first moment at which the point is behind the discontinuity tip.

When a discontinuous kinematic representation is considered in the the rate-dependent elastoplastic damage model, described in Appendix A, the justification for the use of discontinuities stems from a better interpretation of some field quantities which gain a clearer physical meaning. The evolution of the equivalent plastic strain κ ahead of the discontinu-

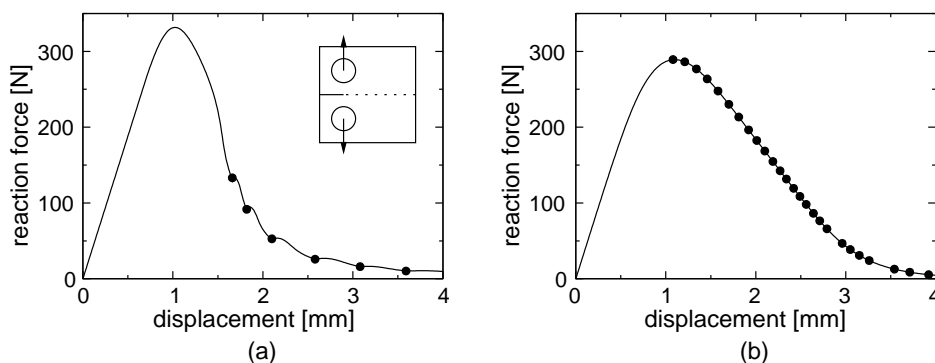


Figure 6: Load-displacement curves for implicit gradient-enhanced continuum damage model (a) and rate-dependent elastoplastic damage model (b) with a propagating discontinuity. The discontinuity propagates from the notch along the dotted line. The dots represent the extension of the discontinuity. Note that the extension is performed through several elements at a time for the gradient-enhanced model and through one element at a time for the rate dependent model.

ity tip is depicted in Figure 7. The propagating discontinuity avoids the artificial growth of

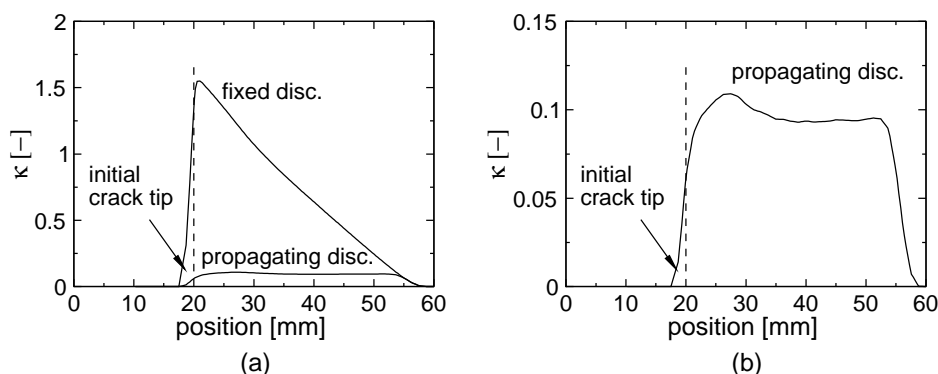


Figure 7: Profile of the equivalent plastic strain κ for the rate-dependent elastoplastic damage model: comparison of profiles with fixed and propagating discontinuity (a) and close-up of the profile in case of propagating discontinuity (b).

the equivalent plastic strain which, in a continuous setting, is the response of the model to strain localisation. It is noted that this is the only observable difference in this model when the continuous and the continuous with transition to continuous/discontinuous models are compared (load-displacement curves and damage profiles are identical).

If the regularised model is unable to describe the narrowing of the degraded zone the inclusion of a traction-free discontinuity is problematic and its use should be avoided. An

example of such a model is the gradient elastoplasticity model [13–15] which is not able to “properly model complete failure” since gradient contributions make it “impossible to reach zero stress values” [16]. A similar problem is to be found in classical viscoplasticity (like *e.g* in Perzyna viscoplasticity) in which the stress-strain relationship presents a horizontal plateau or even an increasing stress due to the viscous stress contribution. When traction-free discontinuities are considered in a rate-dependent viscoplastic model, load-displacement curves exhibit a saw-tooth like shape caused by high residual stresses which have not been dissipated [17] (cf Figure 8).

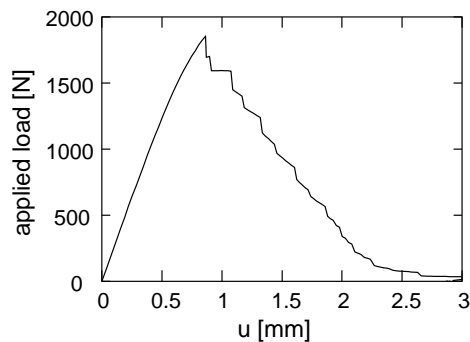


Figure 8: Inclusion of discontinuities in a rate-dependent elastoplastic model: load-displacement response for a biaxial specimen under tensile loading. Adapted from [17].

7 CONCLUSIONS

Some issues related to the use of kinematic discontinuities in regularised media have been discussed. The use of discontinuities can be beneficial in achieving a more realistic representation of failure processes. It was shown that the properties of the underlying regularised continuum play a major role in determining the quality of the discontinuous kinematics enrichment. In particular, the use of discontinuities is beneficial in avoiding spurious dissipation related to non-local regularisation. However, the response of the model to the enhancement is problematic.

A rate-dependent elastoplastic damage model has been described and its regularisation properties have been discussed along with its use in the coupled continuous/discontinuous analysis of failure.

ACKNOWLEDGEMENT

The authors acknowledge the contribution of H. Askes and A. Metrikine (TU Delft) to Section 5 and the stimulating discussions with R.H.J Peerlings and M.G.D. Geers (TU Eindhoven). LJS acknowledges J.F. Georgin (INSA de Lyon) for valuable discussions on

the topic of Appendix A. Financial support to AS through the BEO programme (special fund from TU Delft for excellent research) is gratefully acknowledged.

APPENDIX A

RATE-DEPENDENT ISOTROPIC ELASTOPLASTIC DAMAGE MODEL

A typical feature of rate-dependent plasticity is the inability to achieve full stress relaxation in the load-displacement response. Through the reduction of the stress tensor of the rate-dependence elastoplastic model by the coupling to damage, the load-displacement response converges to a response with no residual load-carrying capacity. The model clearly indicates a narrowing of the degraded zone which corresponds, in the continuum description, to a localised crack.

The rate-dependent isotropic elastoplastic damage model described here is derived from the class of models proposed by Ju [18]. The coupling of damage and plasticity is introduced by adopting the effective stress concept and the hypothesis of strain equivalence. In such a framework, a simple algorithmic formulation, based on the operator splitting technique [19], can be derived. The algorithmic procedure for the coupled model hinges on the stress tensor $\tilde{\boldsymbol{\sigma}}$ and on the algorithmic tangent moduli $\tilde{\mathbf{D}}^p$ in the effective space and on the equivalent plastic strain κ .

A.1 STRESS UPDATE AND ALGORITHMIC TANGENT

The stress update relation at the end of the time step (at t_{n+1}) for the elastoplastic damage model reads

$$\boldsymbol{\sigma}_{n+1} = (1 - \omega_{n+1}) \tilde{\boldsymbol{\sigma}}_{n+1} \quad (\text{A.1})$$

where the damage value is updated through

$$\omega_{n+1} = \alpha (1 - \exp(-\beta \kappa_{n+1})), \quad (\text{A.2})$$

with α and β parameters influencing the asymptotic value of damage and the slope of the damage evolution law, respectively, and κ_{n+1} the equivalent plastic strain in the effective space for the elastoplastic problem.

The algorithmic tangent stiffness tensor \mathbf{D}^{pd} is defined by $d(\Delta\boldsymbol{\sigma}) = \mathbf{D}^{\text{pd}} : d(\Delta\boldsymbol{\varepsilon})$ for variations $d(\Delta\boldsymbol{\varepsilon})$ of the current strain increment $\Delta\boldsymbol{\varepsilon}$. To derive the consistent tangent operator, equation (A.1) is differentiated at t_{n+1} (note that $d(\square_n) = 0 \rightarrow d(\square_{n+1}) = d(\Delta\square)$) to obtain (dropping the subscript $n + 1$):

$$d(\Delta\boldsymbol{\sigma}) = (1 - \omega) d(\Delta\tilde{\boldsymbol{\sigma}}) - d(\Delta\omega) \tilde{\boldsymbol{\sigma}}. \quad (\text{A.3})$$

The rate of change of the damage variable $d(\Delta\omega)$ can be related to $d(\Delta\boldsymbol{\varepsilon})$ by

$$d(\Delta\omega) = \frac{\partial\omega}{\partial\kappa} d\kappa = \frac{\partial\omega}{\partial\kappa} \tilde{b}(\tilde{\boldsymbol{\sigma}}) d\lambda = \frac{\partial\omega}{\partial\kappa} \tilde{b}(\tilde{\boldsymbol{\sigma}}) \tilde{\mathbf{a}} : d(\Delta\boldsymbol{\varepsilon}), \quad (\text{A.4})$$

where $\tilde{b}(\tilde{\boldsymbol{\sigma}})$ is a factor relating the accumulated equivalent plastic strain to the plastic multiplier and $\tilde{\mathbf{a}}$ is a second order tensor which depends on the plasticity model in the effective stress space and which will be specified later. Substituting $d(\Delta\omega)$ from the above expression in equation (A.3), and recalling that $d(\Delta\tilde{\boldsymbol{\sigma}}) = \tilde{\mathbf{D}}^p : d(\Delta\boldsymbol{\varepsilon})$, yields the consistent tangent operator for the elastoplastic damage model:

$$\mathbf{D}^{pd} = (1 - \omega) \tilde{\mathbf{D}}^p - \frac{\partial\omega}{\partial\kappa} \tilde{b} \tilde{\boldsymbol{\sigma}} \otimes \tilde{\mathbf{a}}. \quad (\text{A.5})$$

Note that no restriction has been placed on the nature of the plastic moduli $\tilde{\mathbf{D}}^p$, of the stress tensor $\tilde{\boldsymbol{\sigma}}$ and of the equivalent plastic strain κ which are computed in the effective stress space. However, to preserve well-posedness of the governing equations when softening constitutive relationships are used, a rate-dependent response in the effective stress space must be used.

The Perzyna viscoplastic model [20] has been conveniently chosen for its robustness. In presence of plastic flow ($\tilde{f} \geq 0$, where \tilde{f} is the yield function in the effective stress space), the viscoplastic strain rate for the Perzyna model is expressed in the associative form:

$$\dot{\boldsymbol{\varepsilon}}^{vp} = \frac{1}{\tau} \tilde{\phi} \tilde{f}_{\boldsymbol{\sigma}}, \quad (\text{A.6})$$

where τ is the relaxation time, $\tilde{f}_{\boldsymbol{\sigma}} = \partial\tilde{f}/\partial\tilde{\boldsymbol{\sigma}}$ and the overstress function is given the following power-law form

$$\tilde{\phi}(\tilde{f}) = \left(\frac{\tilde{f}}{\bar{\sigma}_0} \right)^N, \quad (\text{A.7})$$

with $\bar{\sigma}_0$ the initial yield stress and N ($N \geq 1$) a real number. After standard manipulations [21], the algorithmic treatment of the constitutive equations for Perzyna viscoplasticity in the effective stress space yields the rate of change of the incremental plastic multiplier

$$d\lambda = d(\Delta\lambda) = \frac{\tilde{f}_{\boldsymbol{\sigma}} : \tilde{\mathbf{R}} : d(\Delta\boldsymbol{\varepsilon})}{\tilde{f}_{\boldsymbol{\sigma}} : \tilde{\mathbf{R}} : \tilde{f}_{\boldsymbol{\sigma}} - \tilde{f}_{\kappa} \kappa_{\lambda} + \tau / (\Delta t \tilde{\phi}_{\tilde{f}})} \quad (\text{A.8})$$

and the consistent tangent

$$\tilde{\mathbf{D}}^p = \tilde{\mathbf{R}} - \frac{\tilde{\mathbf{R}} : \tilde{f}_{\boldsymbol{\sigma}} \otimes \tilde{f}_{\boldsymbol{\sigma}} : \tilde{\mathbf{R}}}{\tilde{f}_{\boldsymbol{\sigma}} : \tilde{\mathbf{R}} : \tilde{f}_{\boldsymbol{\sigma}} - \tilde{f}_{\kappa} \kappa_{\lambda} + \tau / (\Delta t \tilde{\phi}_{\tilde{f}})} \quad (\text{A.9})$$

where

$$\tilde{\mathbf{R}} = \left(\mathbf{I} + d\lambda \mathbf{D}^e \tilde{f}_{\boldsymbol{\sigma}\boldsymbol{\sigma}} \right)^{-1} \mathbf{D}^e, \quad (\text{A.10})$$

$\square_i = \partial\square/\partial i$, $\tilde{f}_{\boldsymbol{\sigma}\boldsymbol{\sigma}} = \partial\tilde{f}_{\boldsymbol{\sigma}}/\partial\tilde{\boldsymbol{\sigma}}$, \mathbf{I} is the fourth-order identity tensor and \mathbf{D}^e is the fourth-order elastic stiffness tensor. After employing the symmetry of $\tilde{\mathbf{R}}$, the second order tensor

$\tilde{\mathbf{a}}$ (cf equation (A.4)), required for the evaluation of the consistent tangent operator for the elastoplastic damage model in equation (A.5), reads:

$$\tilde{\mathbf{a}} = \frac{\tilde{\mathbf{R}} : \tilde{f}_\sigma}{\tilde{f}_\sigma : \tilde{\mathbf{R}} : \tilde{f}_\sigma - \tilde{f}_\kappa \kappa_\lambda + \tau / (\Delta t \tilde{\phi}_{\tilde{f}})}. \quad (\text{A.11})$$

The consistent tangent operator for the elastoplastic damage model is readily available by direct substitution of the above expressions into equation (A.5). It is noted that the consistent tangent operator is not symmetric. The step-by-step integration procedure is very similar to that of standard plasticity, the difference being the presence of the damage update which requires only the evaluation of equations (A.1) and (A.5).

A.1.1 Influence of model parameters

The influence of the model parameters is studied by considering the integration point level response for Von Mises plasticity by means of a one-element test in displacement control on a 8-node quadrilateral element (element size 1 mm \times 1 mm). The element is subject to monotonic linearly increasing uniaxial loading at constant strain rate ($\Delta t = 0.0001$ s till the final displacement of 0.1 mm is reached). The model parameters adopted are: Young's modulus $E = 100$ MPa and Poisson's ratio $\nu = 0$. The softening rule governing the cohesion capacity of the material is given an exponential form according to:

$$\sigma_y(\kappa) = \bar{\sigma}_0 ((1 + a) \exp(-b\kappa) - a \exp(-2b\kappa)), \quad (\text{A.12})$$

with a and b model parameters. The results of the analyses are shown in Figure A.1. The effective reduction of the residual stress due to damage as in Figures A.1a and A.1b and the effect of the relaxation time τ reported in Figures A.1c and A.1d are worth noting. The effect of the softening rule parameters is depicted in Figures A.1e and A.1f. The constitutive response to a series of loading-unloading-reloading cycles is reported in Figure A.2 along with the response of the model to monotonic loading (model parameters are: $a = 0$, $b = 1$, $\alpha = 1$, $\beta = 100$, $\tau = 0.5$ s).

A.2 REGULARISATION PROPERTIES

The regularisation properties of the model are demonstrated considering a bar of length $L = 100$ mm, thickness $t = 1$ mm and width increasing from 8 mm at the restrained end to 10 mm at the free end. In the finite-element discretisations, the b.c.'s are prescribed restraining both bottom node directions and vertical top node direction. The bar is subjected to monotonic tensile loading with constant average strain rate obtained by increasing the displacement at the free end linearly in time with $\Delta t = 0.0001$ s till the final displacement of 0.1 mm. Von Mises plasticity with yield stress $\bar{\sigma}_0 = 2$ MPa is adopted. Other model parameters are: Young's modulus $E = 24000$ MPa, Poisson's ratio $\nu = 0$, $a = 0$ and $b = 100$ for the exponential softening law parameters of equation (A.12)

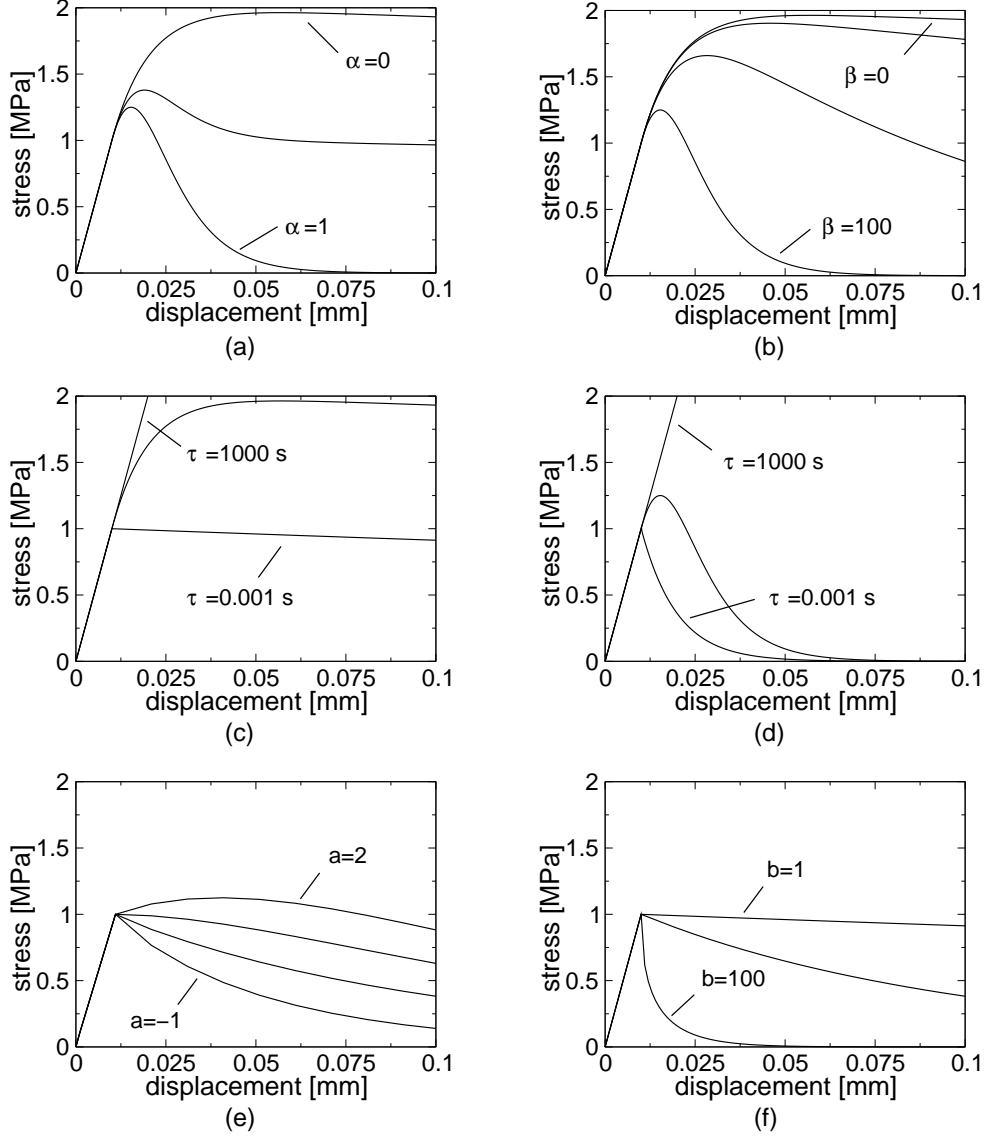


Figure A.1: Influence of the model parameters on the constitutive response: effect of the damage law parameters α with $\alpha = 0, 0.5, 1$ and $\beta = 100$ (a) and β with $\beta = 0, 1, 10, 100$ and $\alpha = 1$ (b) on the rate-dependent elastoplastic damage model ($a = 1, b = 1, \tau = 1$ s); effect of the relaxation time τ with $\tau = 0.001, 1, 1000$ s on the rate-dependent elastoplastic model with $a = \alpha = \beta = 0, b = 1$ (c) and elastoplastic damage model with $a = 0, b = 1, \alpha = 1, \beta = 100$ (d); effect of softening law parameters a with $a = -1, 0, 1, 2$ and $b = 10$ (e) and b with $b = 1, 10, 100$ and $a = 0$ (f) on the rate-independent ($\tau = 0$ s) elastoplastic model.

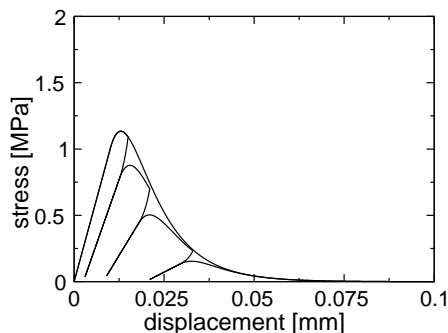


Figure A.2: Response of the model to a series of loading-unloading-reloading cycles compared to a monotonic load response.

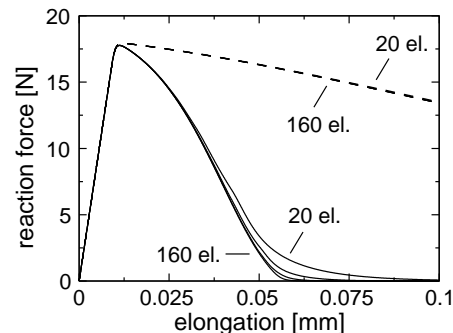


Figure A.3: Load-displacement curves for 20, 40, 80 and 160 element discretisations for the rate-dependent elastoplastic (dashed line) and elastoplastic damage (solid line) model.

and $\alpha = 1$ and $\beta = 300$ for the exponential damage evolution law of equation (A.2). Relaxation time is set to $\tau = 3$ s with $N = 1$ in equation (A.7). It is stressed that these model parameters have been chosen for numerical convenience and that this example is purely academic. Linear quadrilateral elements have been used. The results of the simulations for different discretisations (20, 40, 80 and 160 equally spaced elements) have been reported in Figure A.3 together with the results for the rate-dependent elastoplastic model ($\alpha = \beta = 0$ in the exponential damage evolution law of equation (A.12)). The curves show convergence to a unique solution and the rate-dependent elastoplastic damage model clearly show mesh dependence close to failure due to strain localisation in one element. This is clearer from the stroboscopic evolution plot of the equivalent plastic strain κ reported in Figure A.4 where strain localisation due to damage is evident. The effect of the viscous regularisation is evident from Figures A.5 and A.6 where to a higher relaxation time corresponds a higher energy dissipation and a wider localisation zone. The influence of the coupling of damage to the equivalent plastic strain is reported in Figure A.6. Quadratic rate of convergence was attained in all the simulations. Similar results have been obtained by Georgin et al. [22] with a Duvaut-Lions rate-dependent elastoplastic damage model.

A.3 REMARKS

The model described in this Appendix is endowed with some properties which make it a suitable tool for failure analyses. In contrast to standard rate-dependent elastoplastic models, characterised by a constant width of the localisation zone and by a high residual stress due to the viscous contribution, this rate-dependent elastoplastic damage model allows the progressive narrowing of the localisation zone and full stress relaxation, which can be interpreted as a stress-free crack in a continuous setting.

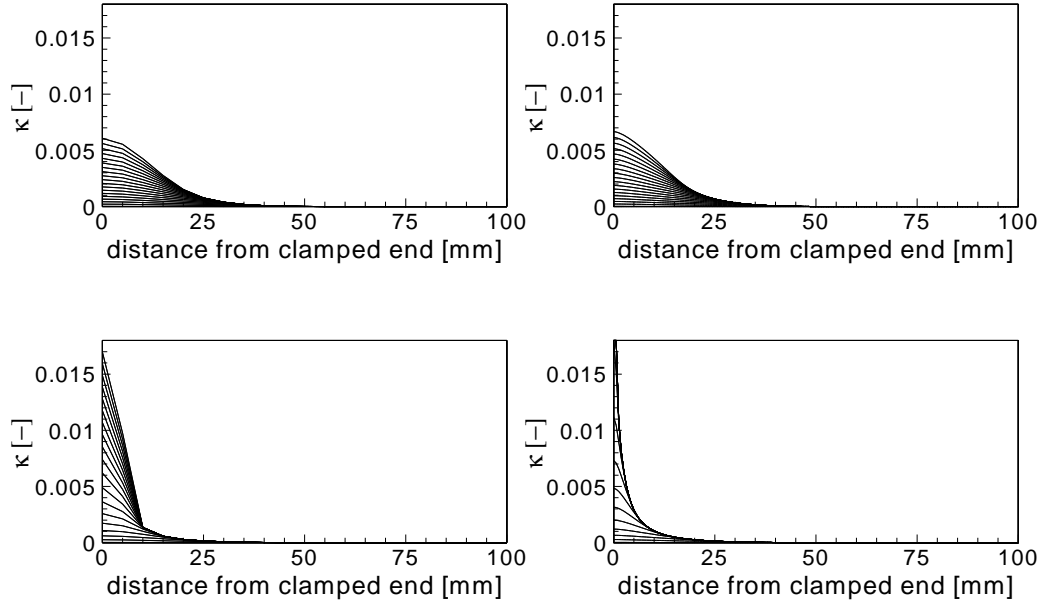


Figure A.4: Stroboscopic evolution of the equivalent plastic strain for the rate-dependent elastoplastic (top) and elastoplastic damage (bottom) model for 20 (left) and 160 (right) element discretisations.

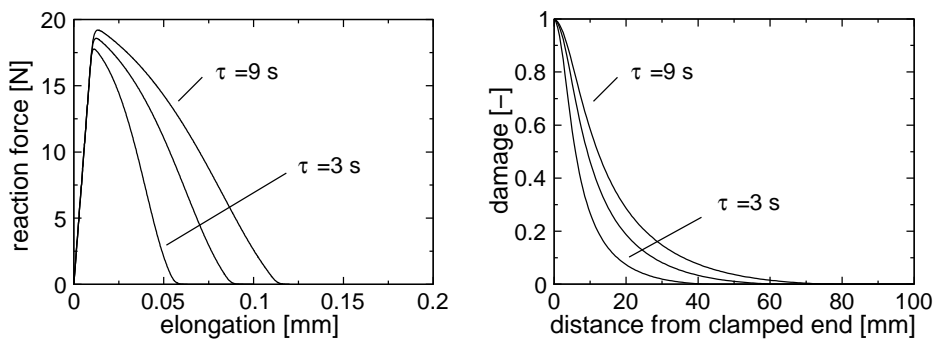


Figure A.5: Effect of the relaxation time on the global response (left) and on damage profile at the end of the computation (right).

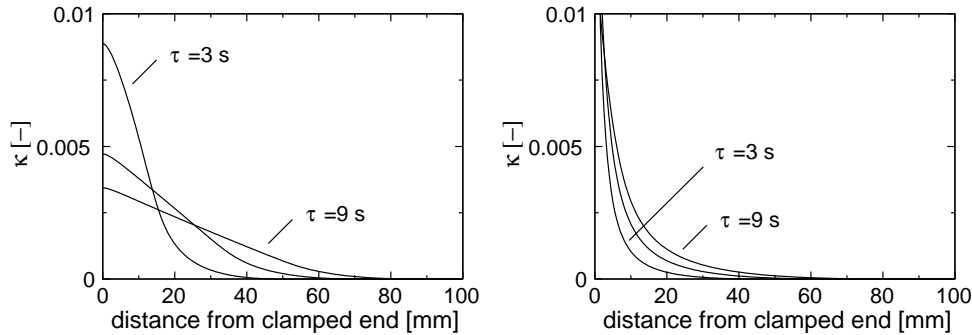


Figure A.6: Effect of the relaxation time on the equivalent plastic strain for the rate-dependent elastoplastic (left) and elastoplastic damage (right) model.

References

- [1] Moës N, Dolbow J, Belytschko T. A finite element method for crack growth without remeshing. *Int. J. Numer. Meth. Engng.* 1999; **46**(1):131–150.
- [2] Wells GN, Sluys LJ. A new method for modelling cohesive cracks using finite elements. *Int. J. Numer. Meth. Engng.* 2001; **50**(12):2667–2682.
- [3] Simone A, Wells GN, Sluys LJ. Discontinuous modelling of crack propagation in a gradient-enhanced continuum. In *Proceedings of the Fifth World Congress on Computational Mechanics (WCCM V)*, HA Mang, FG Rammerstorfer, J Eberhardsteiner, eds. Vienna University of Technology, Austria, volume I 2002; 130.
- [4] Peerlings RHJ, de Borst R, Brekelmans WAM, de Vree JHP. Gradient-enhanced damage for quasi-brittle materials. *Int. J. Numer. Meth. Engng.* 1996; **39**:3391–3403.
- [5] Geers MGD, de Borst R, Brekelmans WAM, Peerlings RHJ. Strain-based transient-gradient damage model for failure analyses. *Comput. Methods Appl. Mech. Engrg.* 1998; **160**:133–153.
- [6] Pamin J, de Borst R. Gradient-enhanced damage and plasticity models for plain and reinforced concrete. In *Proceedings of the European Conference on Computational Mechanics ECCM'99*, W Wunderlich, ed. Technical University of Munich, Munich 1999; 482–483, paper no. 636.
- [7] de Borst R, Pamin J, Geers MGD. On coupled gradient-dependent plasticity and damage theories with a view to localization analysis. *European J. Mech. A/Solids* 1999; **18**(6):939–962.

- [8] Pijaudier-Cabot G, Bažant Z. Nonlocal damage theory. *J. Eng. Mech.* 1987; **113**:1512–1533.
- [9] Eringen AC, Speziale CG, Kim BS. Crack-tip problem in non-local elasticity. *J. Mech. Phys. Solids* 1977; **25**:339–255.
- [10] Hui CY, Riedel H. The asymptotic stress and strain field near the tip of a growing crack under creep conditions. *Int. J. Fract.* 1981; **17**(4):409–425.
- [11] Gao YC, Rousselier G. Near tip quasi-static crack growth behavior in strain hardening and softening material. *J. Theor. Appl. Fract. Mech.* 1994; **20**:149–155.
- [12] Jirásek M, Zimmermann T. Embedded crack model. Part II: Combination with smeared cracks. *Int. J. Numer. Meth. Engng.* 2001; **50**:1291–1305.
- [13] Mühlhaus HB, Aifantis E. A variational principle for gradient plasticity. *Int. J. Solids & Structures* 1991; **28**:845–857.
- [14] de Borst R, Mühlhaus HB. Gradient-dependent plasticity - formulation and algorithmic aspects. *Int. J. Numer. Meth. Engng.* 1992; **35**(3):521–539.
- [15] Pamin J. *Gradient-dependent plasticity in numerical simulation of localisations phenomena*. Ph.D. thesis, Delft University of Technology 1994.
- [16] Engelen RAB, Geers MGD, Baaijens FPT. Nonlocal implicit gradient-enhanced elasto-plasticity for the modelling of softening behaviour. *Int. J. Plast.* 2003; **19**(4):403–433.
- [17] Wells GN. *Discontinuous modelling of strain localisation and failure*. Ph.D. thesis, Delft University of Technology 2001.
- [18] Ju JW. On energy-based coupled elastoplastic damage theories: constitutive modeling and computational aspects. *Int. J. Solids & Structures* 1989; **25**(7):803–833.
- [19] Chorin A, Hughes TJR, McCracken MF, Marsden JE. Product formulas and numerical algorithms. *Commun. Pure Appl. Math.* 1978; **31**:205–256.
- [20] Perzyna P. Fundamental problems in viscoplasticity. In *Advances in Applied Mechanics*, Academic Press, New York, volume 9 1966; 244–368.
- [21] Crisfield MA. *Non-Linear Finite Element Analysis of Solids and Structures: Advanced Topics*. John Wiley & Sons Ltd, Chichester, England 1997.
- [22] Georgin JF, Nechnech W, Sluys LJ, Reynouard JF. A coupled damage-viscoplasticity model for localization problems. In *Proceedings of the Fifth World Congress on Computational Mechanics (WCCM V)*, HA Mang, FG Rammerstorfer, J Eberhardsteiner, eds. Vienna University of Technology, Austria, volume I 2002; 428.